Journal of Alloys and Compounds 519 (2012) 60–66

Contents lists available at SciVerse ScienceDirect

Journal of Alloys and Compounds

journal homepage: www.elsevier.com/locate/jallcom

Characterisation of intermetallic particles formed during solution treatment of an Al–7Si–0.4Mg–0.12Fe alloy

J.Y. Yao*, J.A. Taylor

CAST Cooperative Research Centre (CAST CRC), School of Mechanical and Mining Engineering, The University of Queensland, Brisbane, QLD 4072, Australia

ARTICLE INFO

Article history:
Received 13 September 2011
Received in revised form 8 December 2011
Accepted 12 December 2011
Available online 26 December 2011

Keywords:
Al–Si–Mg cast alloys
Solution treatment
Fe-containing intermetallics
β phase
π phase

ABSTRACT

When Fe-containing Al–7Si–*x*Mg alloys are solution-treated, usually as the initial stage of a T6 heat treatment, some of the π-$Al_9Mg_3FeSi_5$ phase present in the as-cast alloy transforms into fine needle-like intermetallic particles (as seen on a polished surface). These precipitated needles, speculated to be β-Al_5FeSi phase, have not been definitively characterised to date. In this work, electron microscopy characterisation by various techniques was conducted to assess the nature (i.e. the composition, morphology and crystallography) of these particles to verify or otherwise the validity of the above hypothesis. It is found that the particles are indeed β phase platelets, of the same Al_5FeSi or $Al_{4.5}FeSi$ stoichiometry as particles formed during solidification. Close observation of their crystallographic structure suggests fine-scale internal complexities in some of the particles.

1. Introduction

Al–7Si–*x*Mg[1] cast alloys are most commonly used in sand, permanent mould and low pressure die casting processes for the production of load bearing cast components, particularly when the iron impurity content is kept low, such as in primary-sourced aluminium metal. As the iron content increases, there are deleterious effects on both castability and mechanical properties due to the formation of coarse iron-containing intermetallic phases during solidification, most noticeably the β-Al_5FeSi phase. This matter has been extensively reviewed elsewhere [1–4].

The low iron-containing Al–7Si–*x*Mg alloys offer an excellent combination of casting characteristics, machinability and mechanical performance. The properties that enable the high mechanical performance of the components are achieved through heat treatment of the castings, typically a T6 treatment. Two important members of this alloy family are A356 and A357 (following the alloy designations of the Aluminum Association). The former alloy contains ~0.3 wt% Mg while the latter has ~0.6 wt% Mg. The typical T6 treatment for these alloys is a solution treatment for 6 h at 540 °C, followed by warm water quenching and then an artificial ageing treatment at 160 °C for times up to 16 h.

The solution treatment stage achieves three important tasks. Firstly, it causes the break-up of the as-cast eutectic Si phase (which occurs as interconnected flakes in unmodified alloys, and fibrous coral-like structures in modified alloys [5,6]) into small rounded discrete particles [7,8]. Secondly, it causes the dissolution of the Mg-containing micro-constituents (i.e. Mg_2Si and π-$Al_9Mg_3FeSi_5$ phase[2]) thus enriching the Mg and Si content of the aluminium solid solution [7–9]. Thirdly, it homogenizes the distribution of Mg and Si across the dendrite arms of the primary aluminium grains [7,8]. It should be noted that the as-cast β-Al_5FeSi phase (in platelet form) is largely unaffected by the T6 heat treatment, and therefore its deleterious effects are not removed.

Solution treatment prepares the alloy for the subsequent artificial ageing treatment during which fine scale Mg–Si precipitates form that produce the desirable mechanical properties for specific applications. The T6 treatment has been shown to as much as double the hardness and tensile strength and to triple the tensile ductility of gravity cast 356 alloy.

The dissolution process of the Mg_2Si and π-$Al_9Mg_3FeSi_5$ phases in castings of this particular family of alloys has been found to be significantly influenced by the Mg content of the alloy and to a lesser extent by the Fe content and secondary dendrite arm spacing (SDAS) [10–12]. Rometsch et al. [10] found that for alloy 356 (0.3% Mg, 0.2% Fe, SDAS ~40 μm) in the as-cast condition, there is approx. 8 times as much Mg tied up in the π phase as there is in the Mg_2Si phase. When solution treated at 540 °C, the Mg_2Si phase dissolved within 4 min whereas the π phase took 8–15 min to

* Corresponding author. Tel.: +61 7 33653801.
E-mail address: J.Yao@uq.edu.au (J.Y. Yao).

[1] Unless otherwise specified alloy compositions are expressed in wt%.

[2] The π-phase is also commonly given the stoichiometry of $Al_8Mg_3FeSi_6$. However, throughout this paper, the alternative stoichiometry $Al_9Mg_3FeSi_5$ will be used.

0925-8388/$ – see front matter © 2011 Elsevier B.V. All rights reserved.
doi:10.1016/j.jallcom.2011.12.047

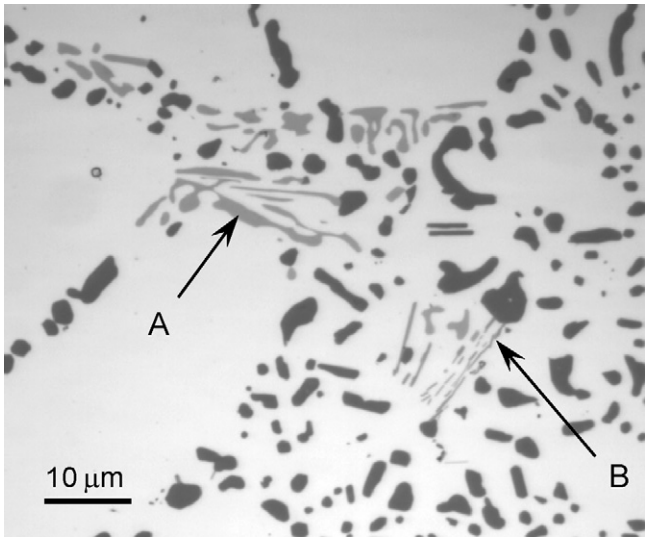

Fig. 1. Optical micrograph showing evidence of the formation of fine needles of β phase (presumed, arrow B) as the Chinese-script π phase (arrow A) dissolves during solution treatment of an Al–7Si–0.4Mg–0.12Fe alloy at 540 °C for 6 h. The image shows different degrees of transformation from partial to nearly complete, in adjacent locations.

dissolve. They also found [10] that for as-cast alloy 357 (0.6% Mg, 0.2% Fe, SDAS ~55 μm), the amount of Mg in the π phase was approx. 2.5 times greater than that in Mg_2Si phase. When the alloy was solution treated at 540 °C for 30–50 min, only half of the Mg_2Si dissolved while the amount of π phase remained largely unchanged.

Associated with the dissolution process of Mg_2Si and π phases during the solution treatment, it has also been observed that an intermetallic phase containing Al, Fe and Si forms as clusters of fine needles (as seen on polished metallographic samples) in same regions where the π phase particles were originally found [12]. The particles appear to progressively grow as more of the π phase dissolves and to precipitate in the free space created after dissolution rather than transform directly from the π phase (Fig. 1). These fine needles were considered to be β-Al_5FeSi phase[3] as suggested by several observations: their needle-like morphology as seen on polished samples in optical microscopy; qualitative compositional assessment by energy dispersive X-ray spectroscopy (EDS) from polished samples; and from phase proportion calculations using Thermo-Calc™ software [11,12]. This consideration was further supported by the results of a mass balance characterisation of phase changes arising from solution treatment of these alloys [10]. However, the crystallographic nature of this precipitated intermetallic phase was not determined to validate the above consideration.

Since the release of Mg atoms from Mg-containing phases to the Al solid solution via solution treatment is crucial for promoting the required response of the alloy to the subsequent artificial ageing treatment, it is important to understand the associated phase changes. In this regard, it was considered necessary to further characterise the microstructural nature of the needle-like intermetallic phase, namely the presumed β-Al_5FeSi, formed in association with the dissolution of Mg_2Si and π phase. Characterisation of as-cast β phase has been previously undertaken, however, a targeted study of this solid state transformation product has not been carried out.

[3] The β-Al_5FeSi intermetallic phase (normally given as either monoclinic or orthorhombic structure) is also frequently designated with an $Al_{4.5}FeSi$ stoichiometry. In this work, the former most common designation is used predominantly. Kral [13] provides a comprehensive review of the various crystallographic designations that have been reported for this phase.

Table 1
Measured composition (wt%) of the selected 356 alloy.

Al	Si	Mg	Fe	Ti	Sr
Bal	7.11	0.40	0.128	0.016	0.01

In this work, analytical transmission electron microscopy (TEM) was conducted to examine the crystal structure of the needle-like phase formed during solution treatment of a 356 alloy containing 0.4% Mg and 0.12% Fe. Furthermore, focused ion beam (FIB) sectioning was performed to enable examination of the morphology of the particles, while EDS was performed in both TEM and SEM (scanning electron microscopy) to assess the composition of the particles.

2. Experimental

The sample material used in this work is taken from alloy 356 plate castings [14] from a region with SDAS ~40 μm. The plate castings were produced using the improved low pressure sand casting process [15] (which provides strong directional solidification conditions by use of a heavy end chill). The melting, alloying and casting procedures are described elsewhere [14,16]. The composition of the investigated alloy, as measured by inductively coupled plasma atomic emission spectroscopy (ICP-AES) is shown in Table 1.

The specific T6 treatment given to this alloy was solution treatment at 540 °C for 6 h, water quenched at 80 °C, and followed immediately by artificial ageing at 160 °C for 8 h.

Samples for SEM/EDS characterisation were prepared following conventional metallographic sample preparation procedures up to a 1 μm diamond polishing finish. They were then carbon coated. The characterisation was performed with a Joel 7001F instrument operating at 15 keV. An FEI™ FIB 200 instrument with a Ga source accelerated at 30 keV was used to perform the micro-sectioning of the intermetallic phases.

Thin foil specimens for TEM observation were prepared from the alloy sample by twin jet electro-chemical polishing with an electrolyte of 75% methanol + 25% nitric acid cooled to −20 °C. The thin foil specimens were then examined in a Joel 2100 TEM instrument operating at 200 keV.

3. Results

3.1. General observation

The needle-like intermetallic particles previously observed to form in alloy 356 during solution treatment have been characterised in this work by various experimental techniques: composition by EDS in both SEM and TEM; morphology by FIB followed by SEM; and crystal structure by TEM.

Fig. 2(a) shows the typical appearance in SEM of the various micro-constituents (Si, π and β) of the Al–7Si–0.4Mg–0.12Fe (356) alloy following solution treatment. Fig. 2(b)–(e) shows associated X-ray maps indicating the partitioning of the alloy elements among the phases.

In Fig. 2(a) it can be seen that the π phase particles, which were of a script-like morphology in the as-cast condition [12] (see also Fig. 1), have been broken up into discrete rounded particles. In the vicinity of, but not necessarily in contact with these rounded π phase particles, some needle-like particles are observed. These are the needle-like particles which Taylor et al. [12] considered to be β phase. The location of the needle-like particles in relation to the π phase particles is indicative of their formation process, most likely dissolution followed by re-precipitation, rather than direct transformation of π to β.

Other needle-like β phase particles were also observed to be present in the microstructure. These are relatively larger in size compared to the fine-scale needles, and are likely to have formed during solidification rather than from the dissolution of π phase particles. The coral like as-cast modified eutectic Si is also broken into rounded particles after the solution treatment. As expected at this composition, no Mg_2Si particles were observable after solution treatment [10]; however, Mg was found bound up in the residual π phase particles.

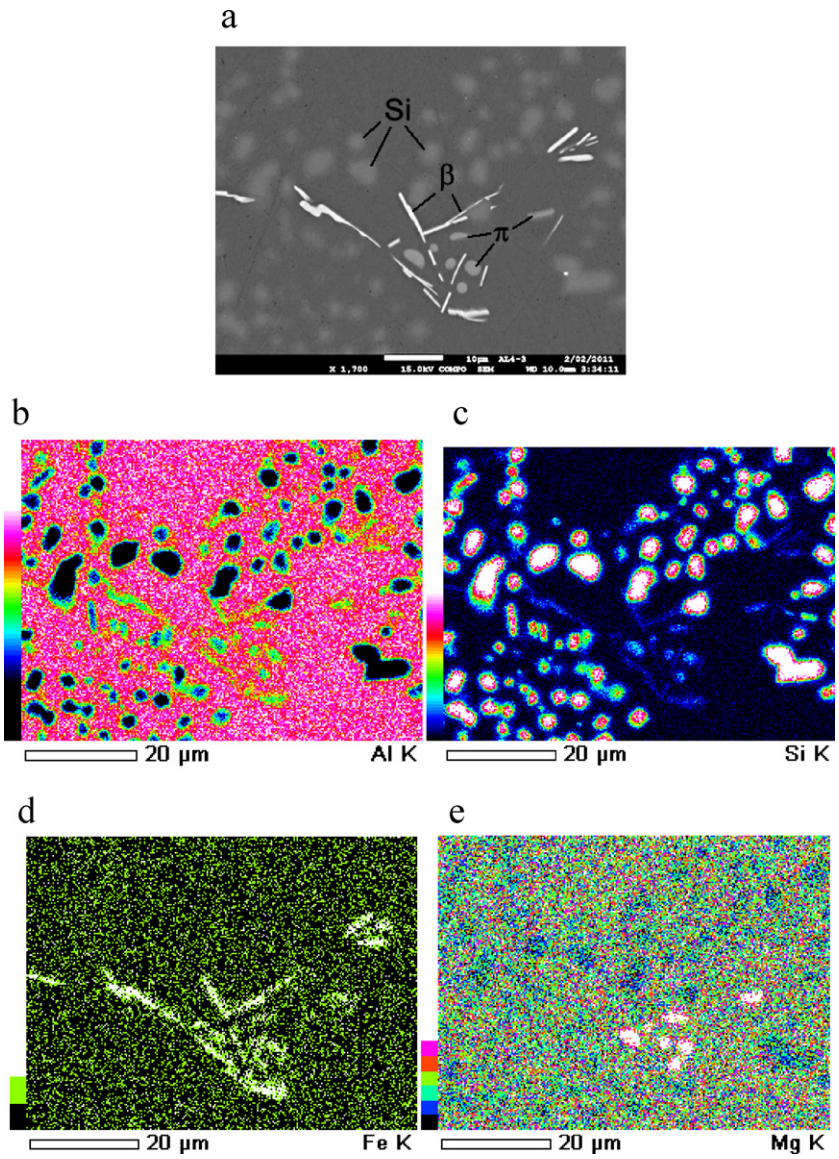

Fig. 2. SEM-EDS mapping of a typical region of cast alloy 356 after solution treatment at 540 °C for 6 h. As marked, the eutectic Si particles have become disconnected and rounded, the π phase has undergone dissolution and has broken up into rounded particles, and some fine β phase particles, as suggested [12], with a needle-like morphology have been precipitated.

3.2. Composition

During TEM examination of the alloy, EDS analyses of the needle-like particles exposed by the electro-chemical polishing process were performed to assess their composition. Fig. 3 is a TEM bright field image showing a cluster of the needle-like particles formed in a region between eutectic Si particles. The results of the EDS analyses of these particles (as numbered in Fig. 3) are shown in Table 2. The relatively small scatter of the EDS results among the various particles indicates that the particles are all of the same composition. The Fe/Si atomic ratio of 1.1 is close to unity (consistent with β-$Al_{4.5}$FeSi or -Al_5FeSi phase [17,18]) while the Al/Si ratio of 3.6 is close to, but lower than the expected 4.5 or 5. It should be noted that the EDS analyses performed here use a standard-less calculation. For composition determination with improved accuracy for these needles in TEM, a thin foil standard with a composition close the current phase would be required.

The compositions of the needle-like particles and the π phase particles, as shown in Fig. 2, were also examined by SEM-EDS. The

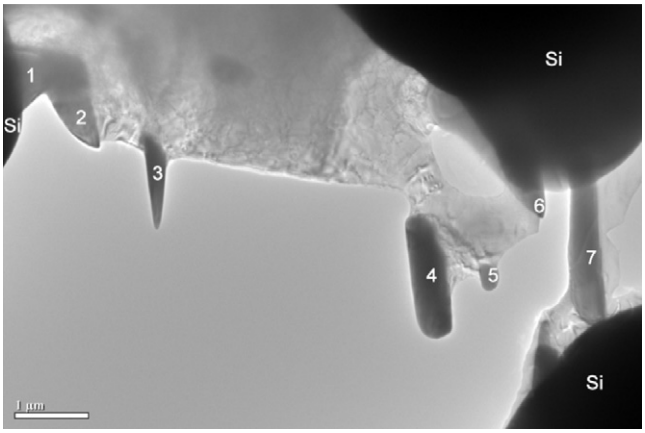

Fig. 3. TEM bright field image of a region containing a number of fine needle-like intermetallic particles formed during the solution treatment of alloy 356. The numbers indicate the particles analysed by EDS (see Table 2).

Table 2
Results of TEM-EDS compositional analyses (atomic %) of the 7 intermetallic particles marked in Fig. 2. Ratios of Fe/Si and Al/Si are also shown.

	Al	Mg	Si	Fe	Ni	Fe/Si	Al/Si
1	61.23	2.78	18.62	17.06	0.26	0.9	3.3
2	61.16	2.75	17.08	18.73	0.23	1.1	3.6
3	61.06	2.30	17.65	18.82	0.14	1.1	3.5
4	61.62	2.99	17.38	17.71	0.14	1.0	3.5
5	60.99	3.15	17.41	18.07	0.31	1.0	3.5
6	62.04	2.95	16.13	18.50	0.29	1.1	3.8
7	61.95	3.04	15.68	19.04	0.23	1.2	4.0
Average	61.4 ± 0.4	2.9 ± 0.3	17.1 ± 1.0	18.3 ± 0.7	0.2 ± 0.1	1.1 ± 0.1	3.6 ± 0.2

results are shown in the plots of Fig. 4. Since the size of these particles was smaller than the size of the interaction volume created by the electron beam in the EDS analysis, the influence of the X-ray counts from the surrounding matrix rather than the particles themselves has to be removed in order to examine the actual composition of the embedded particles. The straight lines of $\Delta Fe/\Delta Si$ and $\Delta Mg/\Delta Si$ shown in the plots are respectively the composition ratios of Fe to Si and Mg to Si for partially embedded particles of β-$Al_{4.5}FeSi$ phase [17] and π-$Al_9Mg_3FeSi_5$ phase [19], with the influence of these elements from the surrounding aluminium matrix removed, after the approach described by Qian et al. [20]. A numerical presentation of the results of these SEM-EDS analyses is shown in Table 3.

From the SEM-EDS analyses shown in Fig. 4 and Table 3, it can be seen that the composition ratio Fe/Si of the needle-like particles is close to that of the normally reported β phase. The composition ratios of Fe/Si and Mg/Si of the rounded π phase are almost identical to those of the less commonly reported π phase stoichiometry, $Al_9Mg_3FeSi_5$ [19].

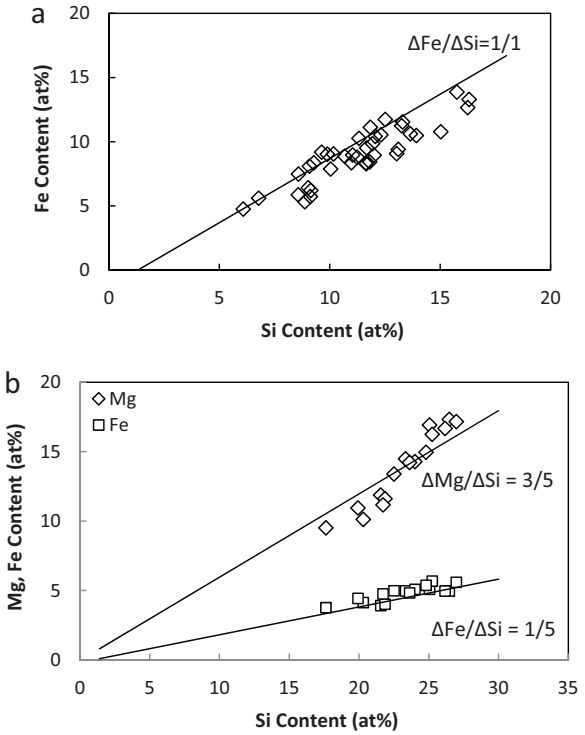

Fig. 4. Plots showing individual analyses from SEM-EDS examination of (a) the needle-like particles, and (b) the rounded π phase particles on a mechanically polished specimen of alloy 356 after the solution treatment. Composition ratio lines of Fe/Si and Mg/Si for partially embedded particles of $Al_{4.5}FeSi$ and $Al_9Mg_3FeSi_5$ phases are shown in (a) and (b) respectively.

Table 3
Results of SEM-EDS analyses of the needle-like particles (39 particles analysed) and the π phase particles (16 particles analysed) in the solution treated 356 alloy. A comparison with known phase stoichiometries is also shown.

	ΔFe/ΔSi	ΔMg/ΔSi
Needle-like particles	0.9 ± 0.1	–
π phase – rounded	0.21 ± 0.01	0.59 ± 0.05
β-$Al_{4.5}FeSi$ phase, or β-Al_5FeSi phase	1	–
π-$Al_9Mg_3FeSi_5$ phase	0.2	0.6
π-$Al_8Mg_3FeSi_6$ phase	0.2	0.5

3.3. Morphology

Fine needle-like shapes observed on two-dimensional polished surfaces are most likely cross-sections of fine platelets existing in three dimensions. In order to verify this consideration, FIB micro-sectioning was performed on some of these needles. A representative SEM micrograph of a FIB cut across the needles is shown in Fig. 5, and clearly illustrates that the fine needles are indeed the cross-sections of fine plate-like particles.

The plate-like morphology is consistent with the morphology of the particles as revealed by TEM. As marked in Fig. 3, particles 1, 2 and 6 have a plate-like shape, particle 3 has a sharpened tip resulting from the electro-chemical polishing, whereas particles 4, 5 and 7 have rounded ends. This range of morphologies suggests that the particles were approximately rounded at the early stage of formation and then preferentially grew along favourable crystallographic directions to result in a final plate-like morphology.

The plate-like morphology of these fine post solution treatment needles, as revealed by FIB and also by TEM, is the same as that observed in situ for β phase particles formed during solidification of aluminium–silicon based alloys using various imaging techniques [21–24].

3.4. Crystal structure

Selected area diffraction in TEM was performed to examine the crystal structure of the needle-like particles. Particles 3, 6 and 7 shown in Fig. 3 were examined by selected area diffraction and, within the error of experiment, all of the diffraction patterns obtained from these particles and the tilting between the diffraction patterns could be indexed consistently according to the Bravais lattices of the β phase as either an A-Centred Monoclinic lattice

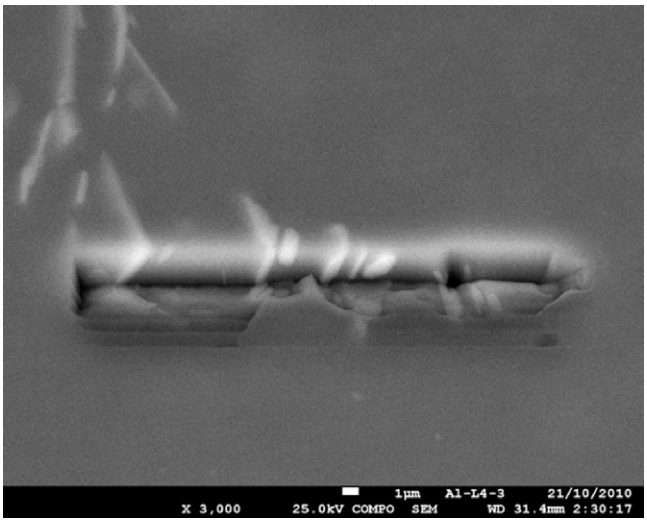

Fig. 5. SEM backscattered electron image showing a FIB cross-section cut through some needle-like particles of alloy 356 after solution treatment. Their morphology is clearly revealed as plate-like.

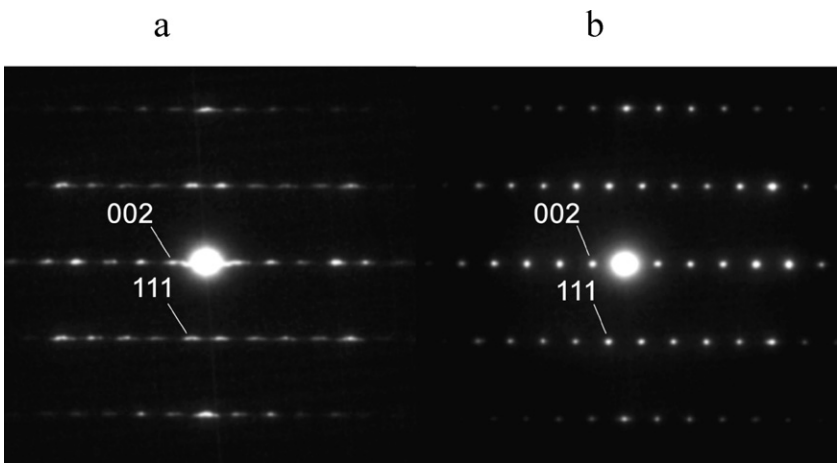

Fig. 6. TEM selected area diffraction patterns of (a) particle 3, and (b) particle 7, as numbered in Fig. 3. Both of the patterns can be indexed as a [$\bar{1}$ 1 0] zone axis pattern of the A-Centred Monoclinic lattice [18]. Note the streaky appearance of each of the reflections along the $\mathbf{g}_{002}$ direction in (a).

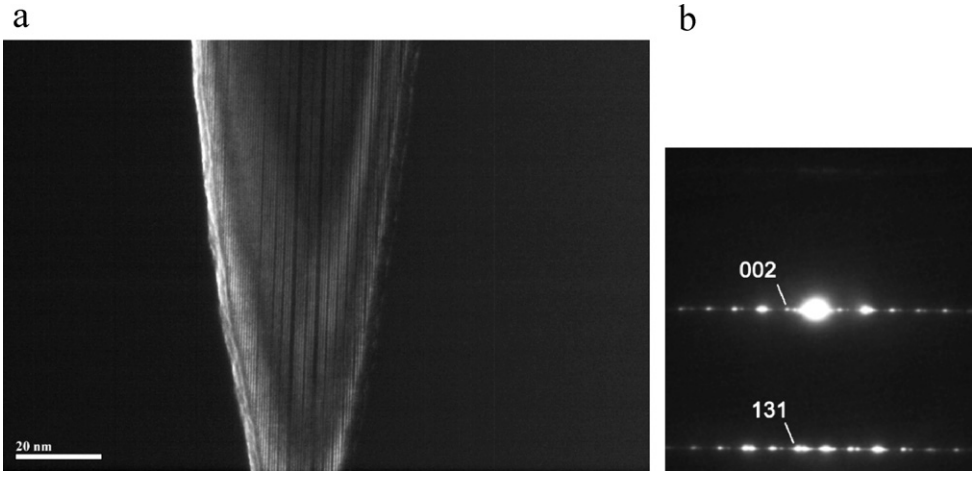

Fig. 7. TEM dark field image taken of the $\mathbf{g}_{002}$ reflection of particle 3 (as marked in Fig. 3) and the associated diffraction pattern, which was indexed as a pattern near the zone axis of [$\bar{3}$ 1 0] of the A-Centred Monoclinic lattice [18]. Note the layered contrast of the (0 0 2) planes in (a) and the broken streaky reflections along the $\mathbf{g}_{002}$ direction in (b).

with $a = 6.161$ Å, $b = 6.175$ Å and $c = 20.813$ Å and $\beta = 90.42^\circ$ [18] or an Orthorhombic lattice with $a = 6.18$ Å, $b = 6.20$ Å and $c = 20.8$ Å [25]. In the following discussion the indexing uses the A-Centred Monoclinic lattice as reference for convenience.

Fig. 6 shows two diffraction patterns taken of particles 3 and 7 (shown in Fig. 3) with the particles being tilted to be imaged along the same zone axis. The diffraction patterns can be consistently indexed as the [$\bar{1}$ 1 0] pattern of the A-Centred Monoclinic lattice [18]. The streak like appearance of the reflections of particle 3 (Fig. 6(a)) indicates that there are fine layered structures on the (0 0 2) planes. This layered structure can be clearly seen in associated dark field images, as shown in Fig. 7.

Close examination of the diffraction patterns of particle 3 shown in both Figs. 6(a) and 7(b) shows that apart from the streaky appearance of the reflections along the $\mathbf{g}_{002}$ direction (which is the normal of the (0 0 2) planes), there are also discrete reflections that appear along the $\mathbf{g}_{002}$ direction around each of the (0 0 2), (1 1 1) and (1 3 1) reflections. These reflections could originate from either the thickness of the layered structure or from a super lattice with increased lattice spacing.[4] The extra reflections observed between the (0 0 2) reflection and the central beam indicate the presence of an additional phase or phases in the particle being analysed. The observation favours the finding by Zheng et al. [25] that there could be more than one phases within the β particle. These phases have nearly identical *a* and *b* lattice parameters but different *c* values with the corresponding axes parallel to each other. The discrete reflections seen in this work are not from the twinning that has been previously observed in the β phase of as-cast alloys [18].

In Fig. 7(a), it can be seen that there are thickness contours evident in the sharp needle shaped particle. There is also obvious dark line contrast running parallel along the length of the needle. The darkness of these lines indicates that the thin layers were in different diffraction conditions from the matrix of the needle. The additional reflections observed in between (0 0 2) and the central beam could originate from these thin layers. The observation of the layered structure on the (0 0 2) planes is consistent with previous findings of the β particle [18,25].

In a word, examination of selected area diffraction patterns of the needle-like particles indicates that their basic crystal structure could be of either of the two crystal structures that have been commonly assigned to the β phase, i.e. monoclinic or orthorhombic. The current analytical method is unable to clearly differentiate between these two crystal structures.

[4] Both of these forms produce extra diffraction reflections around the matrix reflections along the direction of the super-lattice or normal to the fine layers for the layered structure.

4. Discussion

4.1. The dissolution of the π phase and the growth of the β phase

The fact that most of the rounded π phase particles were not in contact with the β phase particles (see Figs. 1 and 2) indicates that the growth of the fine β phase particles is at the expense of the nearby π phase under dissolution and that it does not grow from or transform directly from the π phase. The dissolution of the π phase and the growth of the β phase are most likely to be two individual processes. It is possible that, during solution treatment of the alloy from the as-cast condition, the reduction of Mg content in the matrix around the π phase causes the π phase to dissolve releasing Mg, Si and Fe into the aluminium matrix. Since the diffusion coefficient of Fe in Al is less than one tenth of that of Mg in Al [26], the local Fe content will remain relatively high as the Mg content reduces. This high Fe content will then be a limiting factor for the further dissolution of the π phase. This consideration means that growth of the β phase particles relies on the dissolution of the π phase while concurrently the dissolution of the π phase also needs, to a certain extent, the growth of the β phase to effectively consume the excessive amount of Fe in the surrounding Al matrix.

4.2. Composition measurement

The composition ratios of Fe/Si and Mg/Si as determined by SEM-EDS for the needle-like particles and the rounded π phase after solution treatment is nearly identical to those of the equivalent reported as-cast β phase and π phase. The examination of the composition ratio of the particles rather than the actual compositions of the particles is needed because of the influence of interaction volume induced by the electron beam of 15 keV which is substantially larger than the size of these small particles. This difficulty could be resolved to an extent for these needle-like particles by reducing the energy of the electron beam from 15 keV to, say 7 keV, where the interaction volume will be reduced to submicron sizes well within the width of the needles. However, when the beam energy is reduced, standard-based quantification will become a necessity.

However, the composition of the now-confirmed fine β phase particles may not be uniform because, as was shown by Zheng et al. [25], a tetragonal structured phase appears to coexist within the otherwise monoclinic/orthorhombic crystal structure of the platelets. By employing a composition measurement technique of greater accuracy, such as atom probe, the constitution of the β phase may be better characterised and the role of various alloy additions on the morphology of this β phase better understood.

It is noted in this work that trace levels of Ni were present in the needle-like particles (see Table 2). The origin of this impurity and its role, if any, in the formation of the fine needle-like phase and/or in the dissolution of the π phase is unknown; however, substitution of Fe by other transition metals in Fe-containing intermetallics is not unusual.

4.3. The β phase plates

Previous analytical studies on the β phase have either focussed on particles found in as-cast alloys, e.g. [18], or on unidentified and undifferentiated β particles in T6 treated alloys, e.g. [25]. In this present work, the post-solution treatment, re-precipitated β phase has been targeted for analysis for the first time.

The TEM observation of the fine needle-like particles in this work, seems in part to support the finding of Zheng et al. [25] that they may actually be composite particles consisting of an orthorhombic lattice in conjunction with one or more other phases. It must be noted though, that in the present work, needle-like β particles free of planar defects or layered structure on the (0 0 2) planes have also been observed (e.g. particle 7 of Figs. 3 and 6). Thus more than one type of transformed β particle may exist in the post-solution treatment alloy microstructure.

The needle-like particles (or fine β plates) formed during the solution treatment of the alloy and observed in this present work are thus confirmed to occur as both (i) single crystal particles (with the same stoichiometry and crystallography as the normal as-cast β phase), and (ii) composite micro-constituent particles (with complex internal structures similar to those previously reported by Zheng).

This micro-composite designation indicates that there may be a range of unexplored opportunities for the modification the β phase plates through alloy design, solidification conditions and also via heat treatment.

5. Conclusions

Electron microscopy characterisation using various techniques has been conducted to examine the nature of fine needle-like intermetallic particles formed in association with the dissolution of π phase particles during the solution treatment of alloy 356 (Al–7Si–0.4Mg–0.12Fe). The results of this examination are:

- The composition of the needle-like particles, as studied by EDS in both TEM and SEM is consistent with that of the β phase with the stoichiometry $Al_{4.5}FeSi$.
- The morphology of the needle-like particles, as revealed by FIB cross-sectioning and TEM, is actually plate-like for most of the particles observed.
- The crystal structure of the needle-like particles, as examined by selected area diffraction, can be essentially indexed as either the A-Centred Monoclinic lattice [18] or the Orthorhombic lattice [25].
- The particles appear to co-exist in two distinct forms: single crystal particles and composite micro-constituent particles.

It is concluded in this work that the fine needle-like particles formed during the solution treatment of the 356 type alloy are indeed β phase plates similar to those frequently observed in as-cast aluminium alloys but of much finer sizes, most likely formed by precipitation in the vicinity of the dissolving π phase particles.

Acknowledgement

CAST Cooperative Research Centre (CAST CRC) is established under and is supported in part by the Australian Government's Cooperative Research Centre's Scheme.

References

[1] J.A. Taylor, Cast Metals 8 (4) (1995) 225–252.
[2] A. Couture, American Foundryman's Society International Cast Metals Journal 6 (4) (1981) 9–17.
[3] P.N. Crepeau, Transactions of the American Foundryman's Society 103 (1995) 361–366.
[4] T.O. Mbuya, B.O. Odera, S.P. Ng'ang'a, International Journal of Cast Metals Research 16 (5) (2003) 451–465.
[5] S.D. McDonald, K. Nogita, A.K. Dahle, Acta Materialia 52 (14) (2004) 4273–4280.
[6] G.K. Sigworth, International Journal of Metalcasting 2 (2) (2008) 19–40.
[7] D. Apelian, S. Shivkumar, G. Sigworth, Transactions of the American Foundryman's Society 97 (1990) 727–742.
[8] S. Shivkumar, R. Ricci, D. Apelian, Transactions of the American Foundryman's Society 98 (1991) 913–922.
[9] J.A. Taylor, et al., in: E.A. Starke, T.H. Sanders, W.A. Cassandra (Eds.), 7th International Conference on Aluminium Alloys (ICAA-7), Charlottesville, VI, 2000, pp. 277–282.
[10] P.A. Rometsch, G.B. Schaffer, J.A. Taylor, International Journal of Cast Metals Research 14 (1) (2001) 59–69.
[11] J.A. Taylor, D.H. St.John, M.J. Couper, Aluminum Transactions 4–5 (2001) 111–124.

[12] J.A. Taylor, et al., Aluminum Transactions 4–5 (2001) 95–110.
[13] M.V. Kral, Materials Letters 59 (2005) 2271–2276.
[14] J. Barresi, et al., AFS Transactions 108 (2000), p. Paper 00-117.
[15] R.A. Legge, et al., US Patent 5297611: Casting of metal objects, Comalco Aluminium Ltd., USA (1994).
[16] J.A. Taylor, et al., International Journal of Cast Metals Research 12 (6) (2000) 419–430.
[17] P.J. Black, Philosophical Magazine 46 (375) (1955) 401–409.
[18] C. Romming, V. Hansen, J. Gjonnes, Acta Crystallographica 50B (1994) 307–312.
[19] S. Foss, et al., Acta Crystallographica 59B (2003) 36–42.
[20] M. Qian, et al., Journal of Light Metals 1 (2001) 187–193.
[21] C.M. Dinnis, A.K. Dahle, J.A. Taylor, Scripta Materialia 53 (8) (2005) 955–958.
[22] S. Terzi, et al., Acta Materialia 58 (16) (2010) 5370–5380.
[23] M. Timpel, et al., Acta Materialia 58 (20) (2010) 6600–6608.
[24] J. Wang, et al., Scripta Materialia 60 (7) (2009) 516–519.
[25] J.G. Zheng, R. Vincent, J.W. Steeds, Philosophical Magazine A 80 (2) (2000) 493–500.
[26] Y. Du, et al., Materials Science and Engineering A 363 (1–2) (2003) 140–151.